Journal of the Iranian Chemical Society (2024) 21:1661–1668
https://doi.org/10.1007/s13738-024-03025-7

High-performance nickel oxide–graphene composite as an efficient hybrid supercapacitor

Seyed Ali Hosseini Moradi[1] · **Nader Ghobadi**[1]

Received: 22 December 2022 / Accepted: 8 January 2023 / Published online: 6 May 2024

Abstract

Supercapacitors, thanks to their unique properties, are considered among the main future energy storage systems. However, problems such as low energy density relative to batteries, spontaneous discharge, and low cell voltage have limited their widespread use. In this regard, the development of active and efficient materials is known as a viable solution. Thus, in this study, a hybrid supercapacitor made of nickel oxide and graphene was investigated. Nickel oxide and graphene were synthesized by calcination of nickel hydroxide and electrochemical exfoliation of graphite, respectively. Nickel oxide–graphene composites were synthesized at three levels, including 10, 20 and 30%wt of graphene by a facile hydrothermal-calcination route. The samples were characterized by XRD, FE-SEM, elemental mapping and FTIR tests, and their electrochemical performance was evaluated by electrochemical measurements including CV and EIS tests. The result of the characterization tests confirmed the successful synthesis of nickel oxide, graphene and composites. The results of the electrochemical measurements also showed that the addition of graphene to nickel oxide improved the supercapacitive properties of pure nickel oxide. Improved performance of the composites was attributed to the less aggregation of graphene sheets and their greater conductivity. Based on the results of electrochemical tests, the optimum level of graphene addition was 20%wt and NiO@G20 supercapacitor in 2.0 M KOH medium and a scan rate of 5 $\frac{mV}{s}$ showed a specific capacitance of 915.40 $\frac{F}{g}$, energy density of 31.78 $\frac{Wh}{kg}$ and power density of 2.29 $\frac{kW}{kg}$. Also, NiO@G20 supercapacitor was able to maintain 96.7% of its initial capacitance after 5000 cycles, which shows its high cycle stability. The high and stable activity of NiO@G20 introduces it as a promising and high-performance material for supercapacitor.

Keywords Supercapacitor · Graphene · Nickel oxide · Electrochemical exfoliation

Introduction

In recent years, the world energy demand has increased significantly due to the rapid growth of the world's population and industrial development [1]. To date, fossil fuels have mainly met this increasing global energy demand, but they are non-renewable resources, and there are many environmental concerns about air pollution and global warming caused by their consumption. Such problems have necessitated the search for clean and sustainable energy sources to replace fossil fuels [2, 3]. Renewable energy sources, such as solar and wind energy, are known as suitable alternatives to fossil fuels; however, their intrinsic fluctuations have limited their wide usage [4]. Nevertheless, the development of energy storage and conversion systems could make the exploitation of these resources accessible.

There are various types of energy storage systems, but among them, electrochemical storage and conversion systems, including batteries, supercapacitors, and fuel cells, have received much attention [5]. Among electrochemical storage systems, supercapacitors with high power density, long lifespan, fast charge and discharge, and low cost have many advantages over other systems [6]. However, problems such as low energy density relative to batteries, spontaneous discharge, and cell voltage have limited their broad applications [7]. In this regard, the development of active and efficient materials is known as a viable solution. The supercapacitor materials based on the storage mechanism are divided into electrochemical double-layer supercapacitors, pseudocapacitors and hybrid supercapacitors

✉ Nader Ghobadi
n.ghobadi@malayeru.ac.ir

[1] Department of Physics, Faculty of Science, Malayer University, Malayer, Iran

[8]. Electrochemical double-layer supercapacitors have fast charging and discharge ability but relatively low capacitance. Pseudocapacitors have high specific capacitance but suffer from low cyclability [9]. Hybrid supercapacitors exploit the charge storage mechanism of both electrochemical double-layer supercapacitors and pseudocapacitors, and so have the advantages of both categories and have moderated the disadvantages of each. Therefore, hybrid supercapacitors are known as promising energy storage and conversion systems.

The combination of transition metal oxides and graphene or graphene oxide is one of the most studied ideas in the field of hybrid supercapacitors. In this regard, Sawangphruk et al. [10] applied the MnO_2-rGO composite as a hybrid supercapacitor, which showed a performance much better than MnO_2 and rGO solely. Kumar et al. [11] developed rGO@Co_3O_4/CoO hybrid supercapacitor, which showed a specific capacitance of 276.1 $\frac{F}{gr}$ and long-term stability. In another work, Gao et al. [12] synthesized NiO-rGO composite, which with a specific capacitance of 343 $\frac{F}{gr}$ and high capacitance retention demonstrated a considerable supercapacitive performance. Nevertheless, although these examples and many other studies have proved the high potential of the composites of transition metal oxides and graphene or graphene oxide as active hybrid supercapacitors, there is still a long way to achieve a performance as high as what to meet the real application requirements. Also, there are some problems with the complexity of the synthesis procedures that get in the way of their development. Thus, a need for high-performance materials for efficient hybrid supercapacitors with facile synthesis procedure is felt, which has been addressed in this study.

In this work, nickel oxide–graphene composites were synthesized by a novel and facile procedure and applied as hybrid supercapacitors. Nickel oxide and graphene were synthesized simply by calcination of nickel hydroxide and electrochemical exfoliation of graphite. The composites were synthesized in situ with a facile hydrothermal-calcination method. The characterization results indicated the successful synthesis of nickel oxide, graphene and their composites. Also, electrochemical measurements showed the high performance of the nickel oxide–graphene composite with 20%wt content of graphene (NiO@G20) as an efficient hybrid supercapacitor, which introduces it as a promising material for supercapacitor.

Experimental

Materials

$NiSO_4.6H_2O$, NaOH, Na_2SO_4, graphite sheet (All materials were purchased from Sigma-Aldrich Company and were used as received).

Synthesis procedure

In this study, pure nickel oxide and graphene were synthesized by calcination of nickel hydroxide and electrochemical exfoliation of graphite sheet. The composites were synthesized with a two-step hydrothermal-calcination method. The details have been provided in the following.

Synthesis of graphene

Graphene was synthesized by electrochemical exfoliation of a graphite sheet. In a typical procedure, two graphite sheets were placed parallel to each other in a two-electrode cell. A 0.1 M Na_2SO_4 solution was used as the electrolyte. A constant and DC voltage of 7.0 V was applied to the system. After a while, the graphite sheet (anode) began to exfoliate. The exfoliated product was sonicated for one hour. Then, it was washed with distilled water by multiple time centrifugations at 6500 rpm. Finally, the product was dried in a petri dish at 60° C and then collected.

Synthesis of nickel oxide

Nickel oxide was synthesized by the calcination of nickel hydroxide. Nickel hydroxide was synthesized by a facile precipitation method. Typically, 15 ml of a 0.2 M NaOH solution was added droplet-wise to 155 ml of a 0.1 M $NiSO_4.6H_2O$ solution while stirring. Then, the resulting solution was transferred into a 230 ml Teflon-lined stainless steel autoclave and was heated at 100 ℃ for 24 h. Then, the precipitated product was washed several times with distilled water and dried at 60 °C to result in nickel hydroxide powder. Nickel hydroxide powder was poured into a ceramic crucible and calcined in a furnace at 300 °C for 2 h. After the furnace got cooled, the nickel oxide product was collected.

Synthesis of nickel oxide–graphene composite

Nickel oxide–graphene composites were synthesized in situ by a two-step hydrothermal-calcination method. The synthesis procedure was similar to that of nickel oxide, except that in the synthesis of nickel hydroxide and before the addition of NaOH solution, graphene was added to the $NiSO_4$

solution and got stirred for some hours to obtain a uniform solution and let the Ni^{2+} ions to properly adsorb on and distribute over graphene sheets.

Preparation of electrode

A titanium sheet with a size of 1 cm × 2 cm was used as the substrate. Before preparation of the electrode, the substrate was washed with water, polished with sandpaper and etched with 6 M HCl solution to clean the surface from impurities. Then, an area of 1 cm × 1 cm of Ti sheet got covered with an ink containing sample powder dispersed in 5% wt PVDF binder solution (loading ≈ 5 $\frac{mg}{cm^2}$). Finally, the electrode was dried naturally in the air.

Characterization

The X-ray diffraction (XRD) test was conducted using an Inel EQUINOX 3000 X-ray diffractometer with copper kα irradiation. Field emission scanning electron microscopy (FE-SEM) test was performed using a TESCAN Mira3 microscope. Fourier transform infrared spectroscopy (FTIR) test was carried out using a Thermo Scientific Nicolet iS10 spectrometer.

Electrochemical measurements

Electrochemical measurements were performed using an AUTOLAB potentiostat mostly in a three-electrode system. The fabricated electrode, graphite rod, and Ag/AgCl electrode were used as working, counter, and reference electrodes, respectively. All electrochemical measurements were performed in a 2.0 M KOH medium. The cyclic voltammetry (CV) was conducted in a potential window from 0 to 0.5 V (vs. the Ag / AgCl reference electrode) and at different scan rates between 5 and 100 $\frac{mV}{s}$. The electrochemical impedance spectroscopy (EIS) was carried out in a frequency range from 0.1 Hz to 100 kHz and at an AC potential amplitude of 5 mV. To calculate energy density and power density, a two-electrode cell was used in which the fabricated electrode served as both anode and cathode.

Results and discussion

Characterization

The crystalline structure of the materials was examined by XRD test. Figure 1a shows the XRD pattern of graphite sheet as the precursor for the synthesis of graphene and the graphene synthesized by the electrochemical exfoliation method. The XRD pattern of both graphite and graphene corresponds to the reference card number (ICDD: 00-008-0415) and shows no unspecified peak. Both XRD patterns show an indicator peak at 26° corresponding to the (002) crystalline plane of graphene and graphite [13]. As can be seen in Fig. 1a, the characteristic peak of graphene is broader and less intense than that of graphite, indicating the smaller crystallite size and fewer layers of graphene compared with graphite. To investigate this matter quantitatively, the crystallite size of the graphite and graphene was calculated with the Scherer equation (Eq. 1) [14].

$$D = \frac{0.9\lambda}{\mathrm{Cos}(\theta)\beta} \quad (1)$$

where D, λ, θ and β are the average crystallite size, the wavelength of the radiation, Bragg's angle and line broadening at half the maximum intensity, respectively. The crystallite sizes of graphite and graphene were obtained at 24.96 and 3.17 nm, respectively, which confirms the latter assertion. The number of layers of graphite and graphene was determined using XRD results. For this purpose, the thickness of single-layer graphene was considered to be 0.33 nm and by dividing the crystallite size by this value, the number of layers was calculated [15, 16]. Based on this assumption, the number of layers for graphite and graphene was calculated at 76 and 10, respectively. This result shows the high efficiency of the electrochemical exfoliation method and the good quality of the synthesized graphene in terms of thickness and number of layers.

Figure 1b shows the XRD pattern of nickel hydroxide and nickel oxide. The XRD pattern of nickel hydroxide is matched with the standard $Ni(OH)_2$ reference pattern (ICDD: 00-014-0117) and there is no unknown peak related to impurities. The XRD pattern of nickel oxide is also well-matched with the standard NiO reference pattern (ICDD: 01-078-0423) and no peak related to nickel hydroxide is seen, indicating the complete and successful conversion of nickel hydroxide to nickel oxide. The crystallite size of plane (200) of nickel oxide with the highest intensity was obtained at 3.51 nm by using the Scherer equation, which could signify its very small particle size.

Figure 1c shows the XRD pattern of the NiO–graphene composite (NiO@G20). The XRD pattern contains peaks of both nickel oxide and graphene, which confirms the successful synthesis and formation of the composite (the star and the circle represent the peak related to graphene and nickel oxide, respectively).

The functional groups of graphene were investigated by the FTIR test. Figure 1d shows the FTIR spectrum of graphene. The intense and wide peak at 3446 cm^{-1} [1] is related to the stretch of the O–H bond and the peak at 1638 cm^{-1} corresponds to the bending of the O–H bond that both arise from the absorbed water. The peaks at 1115

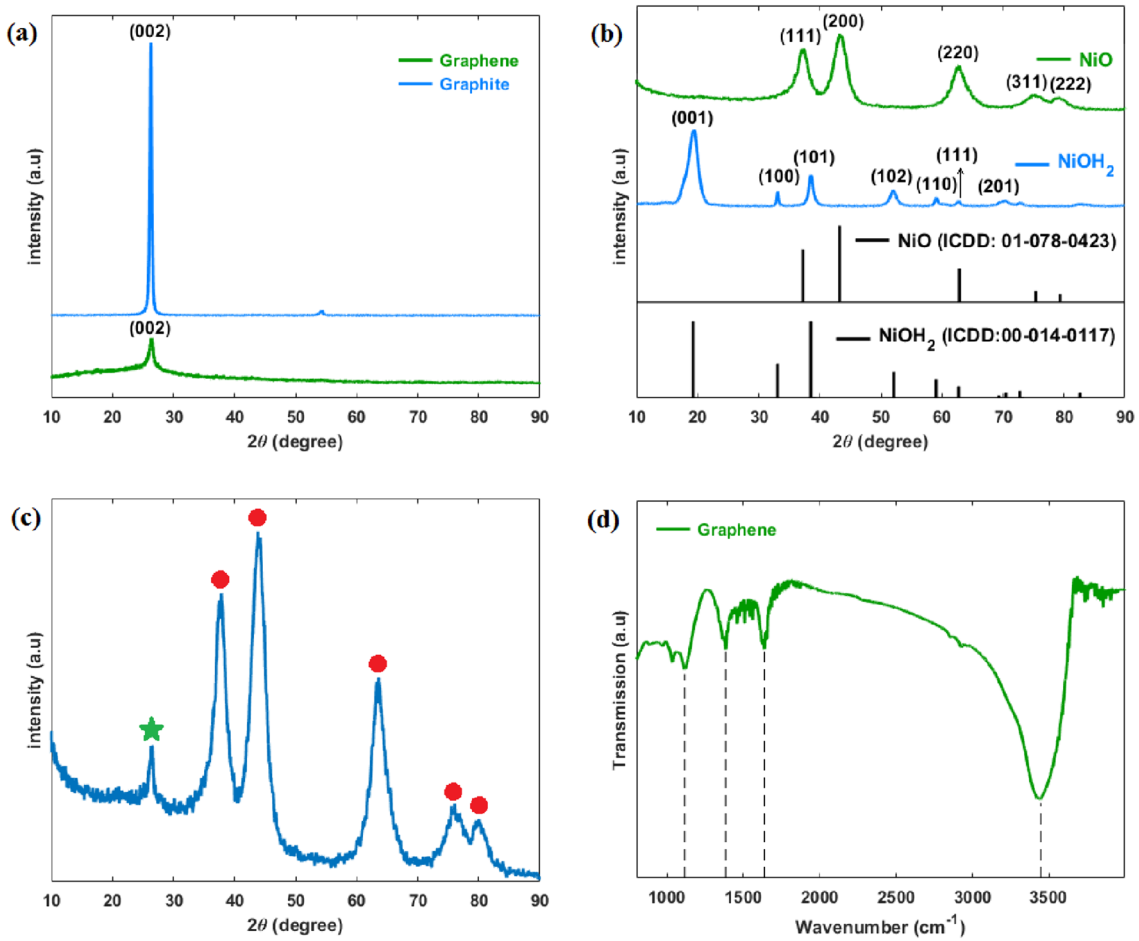

Fig. 1 **a** XRD pattern of graphite and graphene, **b** XRD pattern of nickel hydroxide and nickel oxide, **c** XRD pattern of nickel oxide–graphene composite (the star and the circle represent the peak related to graphene and nickel oxide, respectively) and **d** FTIR spectrum of graphene

and 1384 cm^{-1} could be attributed to the stretch of the C-O bond and the bending of the C-H bond [16.]. Based on this result, as there are almost no oxygen-containing functional groups, the exfoliated graphite could be called graphene rather than graphene oxide.

The morphology of samples was observed with FE-SEM images. Figure 2 shows the FE-SEM images of NiO with 20%wt graphene. A graphene sheet with nickel oxide particles on it obvious is seen. The distribution of elements on the surface of the sample was investigated by elemental mapping. Figure 2 shows the elemental mapping of the NiO with 20%wt graphene. According to elemental mapping, it is obvious that the elements including C, O and Ni have been uniformly distributed on the surface of the sample.

Electrochemical measurements

The nickel oxide–graphene composites were synthesized at three levels, including 10, 20 and 30 wt% and were named NiO@G10, NiO@G20 and NiO@G30, respectively. The electrochemical performance and charge storage mechanism of supercapacitors were investigated by CV test in 2.0 M KOH medium and at ambient temperature. Figure 3 shows the CV curve of all supercapacitors including NiO, NiO@G10, NiO@G20 and NiO@G30 at a scan rate of 5 $\frac{mV}{s}$. According to Fig. 3, the CV curve of NiO has shown a pair of peaks related to redox reactions, indicating that the charge storage mechanism of NiO supercapacitor is pseudocapacitance [17]. When the graphene was added to NiO, the CV curves become somewhat linear, indicating that it is a sign of the electrochemical double-layer charge storage mechanism. Based on this observation, it could be asserted that the charge storage mechanism of NiO@G10, NiO@G20 and NiO@G30 supercapacitors is both electrochemical double-layer capacitance and pseudocapacitance and as a result, they could be considered hybrid supercapacitors [18, 19].

Up to now, the CV curves and electrochemical behavior of the samples were addressed qualitatively. To quantitatively evaluate the supercapacitive performance of the samples, the CV test was performed at different scan rates

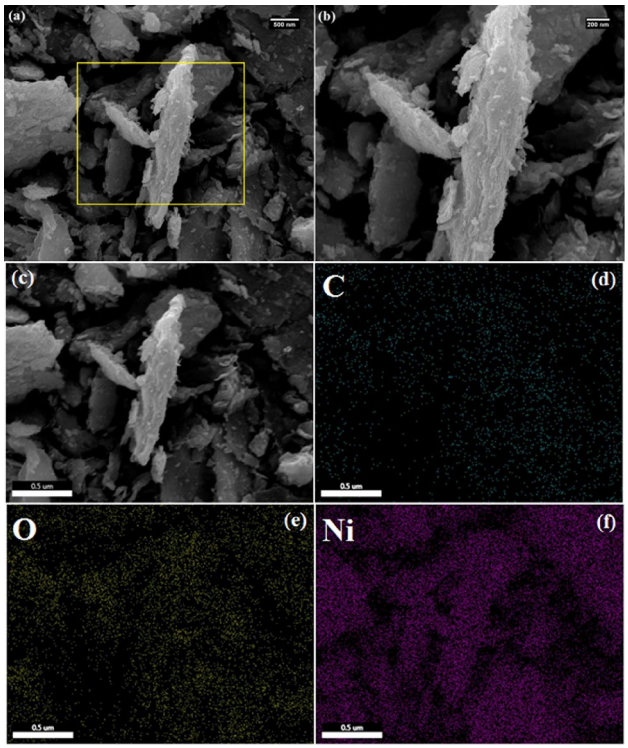

Fig. 2 **a** and **b** FE-SEM image and **c**-**f** elemental mapping of NiO with 20%wt graphene

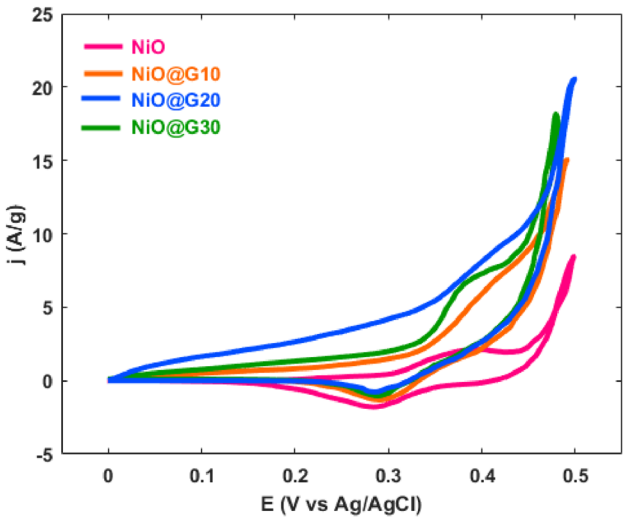

Fig. 3 CV curve of NiO, NiO@G10, NiO@G20 and NiO@G30 in 2.0 M KOH and at scan rate of 5 $\frac{mV}{s}$

from 5 to 100 $\frac{mV}{s}$ for all samples. Figure 4 shows the CV curves of all samples at different scan rates.

Based on Fig. 4, the specific capacitance was calculated from Eq. 2:

$$C_m = \frac{\oint j.\mathrm{dE}}{s.\Delta E} \quad (2)$$

where C_m, j, E and s stand for the specific capacitance, specific current, potential and scan rate, respectively, and $\oint j.\mathrm{dE}$ and ΔE represent the area inside the CV curve and the potential window of the CV test, respectively. Figure 5a shows the specific capacitance as a function of the scan rate for different samples.

As can be seen in Fig. 5a, the specific capacitance of all samples has been decreased with increasing scan rate. This is because as the scan rate increases, there is not enough time for diffusion and storage of charges, resulting in less capacitance. Figure 5b compares the specific capacitance of samples at a scan rate of 5 $\frac{mV}{s}$. Composite samples generally have shown a greater specific capacitance than pure NiO. This observation could be attributed to the synergistic effects of nickel oxide and graphene arising from the combination of electrochemical double-layer and pseudocapacitance mechanisms [20]. Anyway, NiO@G20 composite had the highest capacity in all scan rates and showed a specific capacitance of 915.40 $\frac{F}{g}$ at a scan rate of 5 $\frac{mV}{s}$ and NiO, NiO@G10 and NiO@G30 with a specific capacitance of 389.57, 476.01 and 610.76 $\frac{F}{g}$ respectively, at the same scan rate were placed in the next ranks.

The energy density (E_m) of the samples was calculated using the following equation.

$$E_m = \frac{1}{2} C_m \Delta \mathrm{E}^2$$

Using the above equation and the values obtained for specific capacitance at a scan rate of 5 $\frac{mV}{s}$ in a two-electrode cell, the energy density of samples obtained as presented in Fig. 5c. According to Fig. 5b, NiO, NiO@G10, NiO@G20 and NiO@G30 had specific energy of 13.52, 16.53, 31.78 and 21.10 $\frac{Wh}{kg}$, respectively. It is obvious that NiO@G20 with the highest energy density again performed better than other samples in terms of energy density, which means that it can store more electrical energy per mass unit.

The specific power of the samples was calculated from dividing the specific energy by the charging time. Figure 5d compares the specific power of samples. The specific power of NiO, NiO@G10, NiO@G20 and NiO@G30 were 0.97, 1.19, 2.29 and 1.52 $\frac{kW}{kg}$, respectively. Based on the power density values, it can be seen that the NiO@G20 with the highest power density again had a better performance in terms of power density than other samples.

The charge transfer behavior of supercapacitors was evaluated by the EIS test. The EIS plot of supercapacitors is shown in Fig. 6. As can be seen in Fig. 6, the EIS plot of composites with smaller diameters shows higher conductivity than pure nickel oxide. This improved conductivity

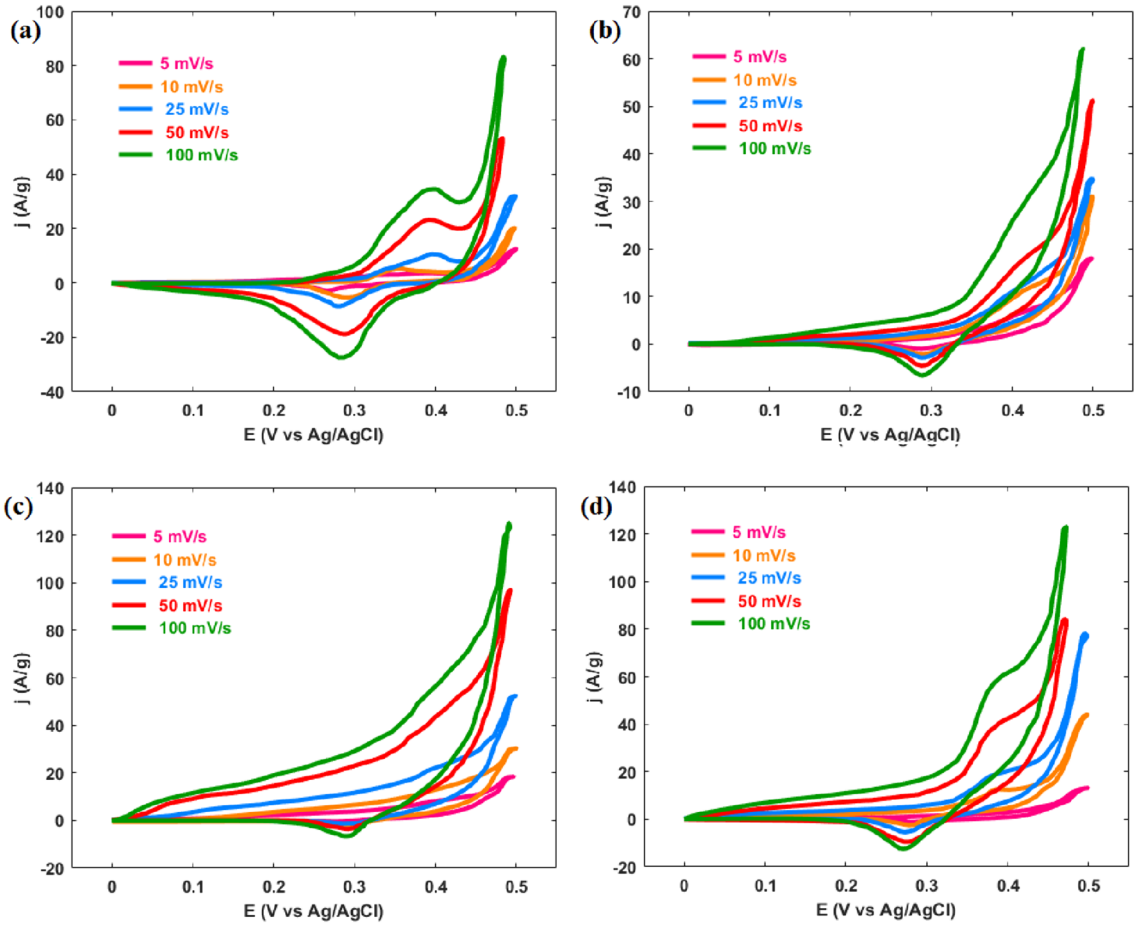

Fig. 4 CV curve of samples at different scan rates: **a** NiO, **b** NiO@G10, **c** NiO@G20 and **d** NiO@G30

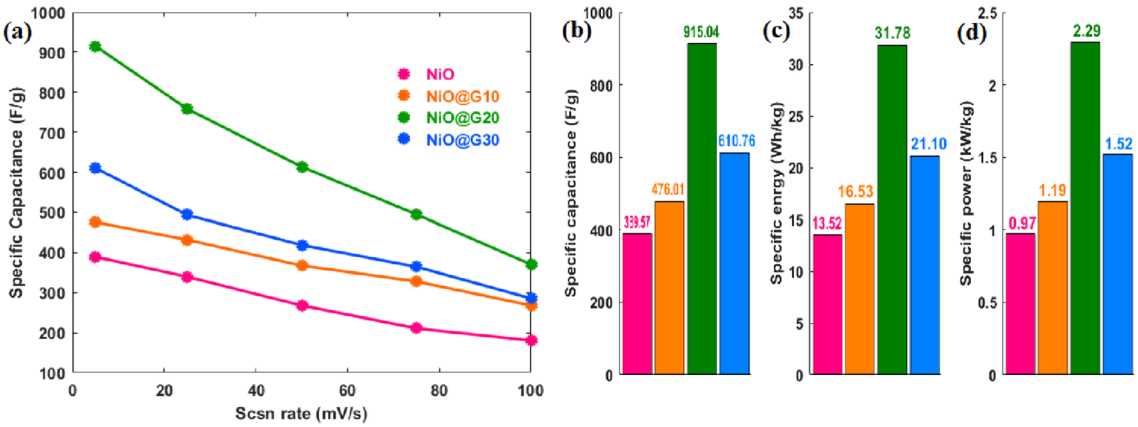

Fig. 5 **a** specific capacitance at different scan rates for different samples, **b** specific capacitance of samples at scan rate of 5 $\frac{mV}{s}$, **c** specific energy of samples and **d** specific power of samples

is due to the higher intrinsic conductivity of graphene than nickel oxide. It can also be seen that NiO@G20 has lower charge transfer resistance than other samples and its better supercapacitive performance can be somewhat attributed to its higher conductivity. The higher conductivity of NiO@G20 than other composites could be attributed to the less aggregation of graphene sheets in this composition. To dipper examine the EIS plots, an equivalent circuit was

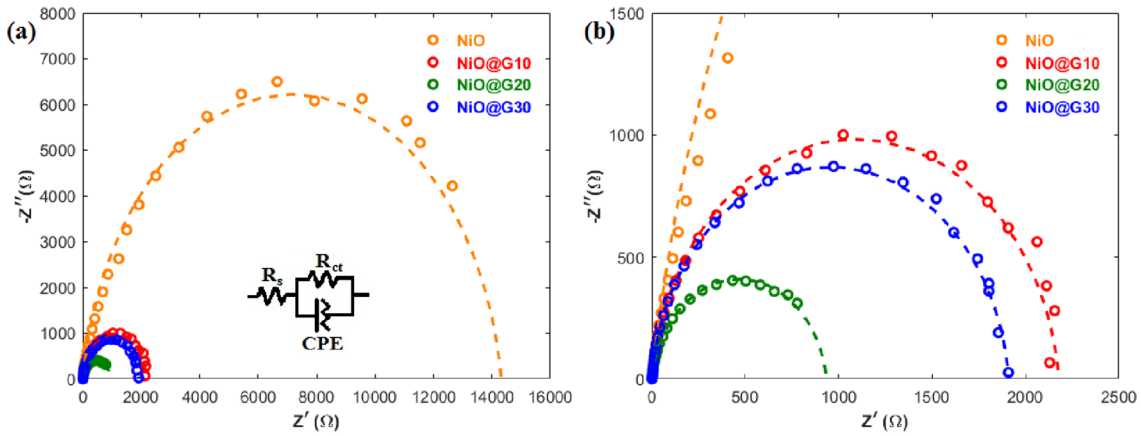

Fig. 6 **a** EIS plot of samples and **b** high-resolution EIS plot of sample

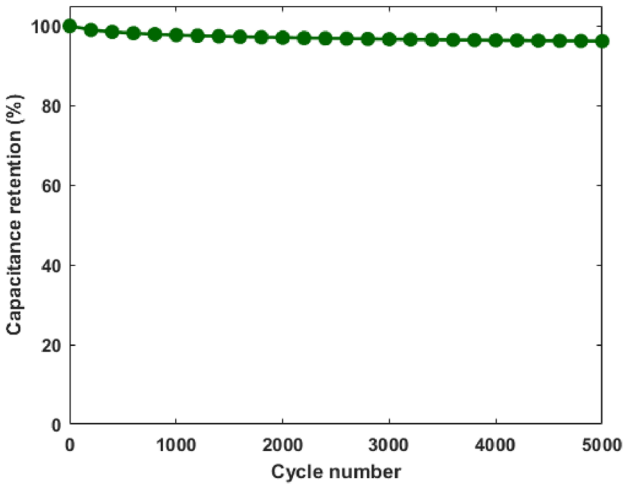

Fig. 7 Cycle stability test of NiO@G20 in a potential window between 0 and 0.5 V

considered (the equivalent circuit is shown in Fig. 6a). By fitting the experimental data with this equivalent circuit, the values of elements in the circuit were obtained. The charge transfer resistance of NiO, NiO@G10, NiO@G20 and NiO@G30 were obtained 14,319, 2176, 933 and 1907 Ω, respectively. According to these values, the improved conductivity of composites compared to pure NiO and the less charge transfer resistance of NiO@G20 than other samples also was corroborated quantitatively.

Based on the provided results, NiO@G20 supercapacitor showed the highest supercapacitive activity. So, to evaluate its lifespan, its cycle stability was also examined. The cycle stability of NiO@G20 was assessed by performing many continuous CV tests in a potential window between 0 and 0.5 V. Figure 7 shows the result of the cycle stability test. According to Fig. 7, the NiO@G20 supercapacitor was able to maintain 96.7% of its initial capacitance after 5000 cycles, indicating its high cycle stability and long lifespan.

Table 1 Comparison of the best sample of the present study with similar studies

	$C_m(\frac{F}{g})$	$E_m(\frac{Wh}{kg})$	$P_m(\frac{kW}{kg})$	References
NiO@G20	915.4	31.78	2.29	Present study
Ru/MnOx/rGO	641	22.3	0.17	[21]
MnO2/N-doped rGO	295.5	24.2	0.24	[22]
V2O5/rGO	612.5	45.9	0.9	[23]

Considering all the results, it can be said that the addition of graphene to nickel oxide by exploiting the benefits of both electrochemical double-layer and pseudocapacitance mechanisms, improving the conductivity through intercalation of graphene sheets enhanced the performance of pure nickel oxide. The optimum percentage of graphene was 20%wt and NiO@G20 supercapacitor with the highest activity was the best sample, which also showed stable long-term performance. Table 1 compares the best sample of the present study with some similar works, where it could be clearly seen that NiO@G20 have shown notable performance in comparison to other studies.

Conclusion

In this study, a hybrid supercapacitor of nickel oxide and graphene was investigated. The nickel oxide and graphene were synthesized by calcination of nickel hydroxide and electrochemical exfoliation of graphite sheet. NiO@graphene composites with 10, 20 and 30%wt content of graphene were synthesized in situ by a two-step hydrothermal-calcination procedure. The samples were characterized by XRD, FE-SEM, elemental mapping and FTIR. The

electrochemical behavior was evaluated by electrochemical measurements, including CV and EIS. The results of the characterization tests confirmed the successful synthesis of nickel oxide, graphene and composites. The results of electrochemical measurements showed that the addition of graphene to nickel oxide improved the supercapacitive properties of pure nickel oxide. Improved performance of composites was attributed to the combination of electrochemical double-layer and pseudocapacitance mechanisms, less aggregation of graphene sheets and higher conductivity. Based on the results of electrochemical tests, the optimum composition was 20%wt of graphene and NiO@G20 supercapacitor in 2 M KOH medium and a scan rate of 5 $\frac{mV}{s}$ showed a specific capacitance, energy density and power density of 915.40 $\frac{F}{g}$, 31.78 $\frac{Wh}{kg}$ and 2.29 $\frac{kW}{kg}$. Also, NiO@G20 supercapacitor was able to maintain 96.7% of its initial capacitance after 5000 cycles, which showed its high cycle stability. The high and stable activity of NiO@G20 introduces it as a promising material for supercapacitor.

Declarations

Conflicts of interest There are no conflicts to declare.

References

1. A.P. Murthy, J. Theerthagiri, J. Madhavan, K. Murugan, Electrodeposited carbon-supported nickel sulfide thin films with enhanced stability in acid medium as hydrogen evolution reaction electrocatalyst. J. Solid State Electrochem. **22**(2), 365–374 (2018)
2. G. Tang, Y. Zeng, B. Wei, H. Liang, J. Wu, P. Yao, Z. Wang, Rational Design of manganese cobalt phosphide with yolk-shell structure for overall water splitting. Energ. Technol. **7**(6), 1900066 (2019)
3. Y. Ge, J. Chen, H. Chu, P. Dong, S.R. Craig, P.M. Ajayan, M. Ye, J. Shen, Urchin-like CoP with controlled manganese doping toward efficient hydrogen evolution reaction in both acid and alkaline solution. ACS Sustain. Chem. Eng. **6**(11), 15162–15169 (2018)
4. J.F. Callejas, C.G. Read, C.W. Roske, N.S. Lewis, R.E. Schaak, Synthesis, characterization, and properties of metal phosphide catalysts for the hydrogen-evolution reaction. Chem. Mater. **28**(17), 6017–6044 (2016)
5. N. Choudhary, C. Li, J. Moore, N. Nagaiah, L. Zhai, Y. Jung, J. Thomas, Asymmetric supercapacitor electrodes and devices. Adv. Mater. **29**(21), 1605336 (2017)
6. X. Cui, R. Lv, R.U. Sagar, C. Liu, Z. Zhang, Reduced graphene oxide/carbon nanotube hybrid film as high performance negative electrode for supercapacitor. Electrochim. Acta **1**(169), 342–350 (2015)
7. C. Liu, Z. Yu, D. Neff, A. Zhamu, B.Z. Jang, Graphene-based supercapacitor with an ultrahigh energy density. Nano Lett. **10**(12), 4863–4868 (2010)
8. Z.S. Iro, C. Subramani, S.S. Dash, A brief review on electrode materials for supercapacitor. Int. J. Electrochem. Sci. **11**(12), 10628–10643 (2016)
9. X. Zang, C. Sun, Z. Dai, J. Yang, X. Dong, Nickel hydroxide nanosheets supported on reduced graphene oxide for high-performance supercapacitors. J. Alloy. Compd. **691**, 144–150 (2017)
10. M. Sawangphruk, P. Srimuk, P. Chiochan, A. Krittayavathananon, S. Luanwuthi, J. Limtrakul, High-performance supercapacitor of manganese oxide/reduced graphene oxide nanocomposite coated on flexible carbon fiber paper. Carbon **60**, 109–116 (2013)
11. R. Kumar, R.K. Singh, R. Savu, P.K. Dubey, P. Kumar, S.A. Moshkalev, Microwave-assisted synthesis of void-induced graphene-wrapped nickel oxide hybrids for supercapacitor applications. RSC Adv. **6**(32), 26612–26620 (2016)
12. X. Gao, H. Zhang, E. Guo, F. Yao, Z. Wang, H. Yue, Hybrid two-dimensional nickel oxide-reduced graphene oxide nanosheets for supercapacitor electrodes. Microchem. J. **164**, 105979 (2021)
13. H. Aghamohammadi, R. Eslami-Farsani, An experimental investigation on the sulfur and nitrogen co-doping and oxidation of prepared graphene by electrochemical exfoliation of pencil graphite rods. Ceram. Int. **46**(18), 28860–28869 (2020)
14. R. Norouzbeigi, M. Edrissi, Preparation of nano alumina powder via combustion synthesis: porous structure optimization via Taguchi L16 design. J. Am. Ceram. Soc. **94**(11), 4052–4058 (2011)
15. M. Coroş, F. Pogăcean, M.C. Roşu, C. Socaci, G. Borodi, L. Mageruşan, A.R. Biriş, S. Pruneanu, Simple and cost-effective synthesis of graphene by electrochemical exfoliation of graphite rods. RSC Adv. **6**(4), 2651–2661 (2016)
16. J.Q. Liu, W. Zhao, G.L. Wen, J. Xu, X. Chen, Q. Zhang, Y. Wang, Y. Zhang, Y.C. Wu, Hydrothermal synthesis of well-standing δ-MnO2 nanoplatelets on nitrogen-doped reduced graphene oxide for high-performance supercapacitor. J. Alloy. Compd. **787**, 309–317 (2019)
17. Y. Zhu, C. Cao, S. Tao, W. Chu, Z. Wu, Y. Li, Ultrathin nickel hydroxide and oxide nanosheets: synthesis, characterizations and excellent supercapacitor performances. Sci. Rep. **4**(1), 1–7 (2014)
18. L. Lai, R. Li, S. Su, L. Zhang, Y. Cui, N. Guo, W. Shi, X. Zhu, Controllable synthesis of reduced graphene oxide/nickel hydroxide composites with different morphologies for high performance supercapacitors. J. Alloy. Compd. **15**(820), 153120 (2020)
19. Z.S. Iro, C. Subramani, S.S. Dash, A brief review on electrode materials for supercapacitor. Int. J. Electrochem. Sci. **11**(12), 10628–10643 (2016)
20. W. Li, Y. Bu, H. Jin, J. Wang, W. Zhang, S. Wang, J. Wang, The preparation of hierarchical flowerlike NiO/reduced graphene oxide composites for high performance supercapacitor applications. Energy Fuels **27**(10), 6304–6310 (2013)
21. K.P. Annamalai, X. Zheng, J. Gao, T. Chen, Y. Tao, Nanoporous ruthenium and manganese oxide nanoparticles/reduced graphene oxide for high-energy symmetric supercapacitors. Carbon **1**(144), 185–192 (2019)
22. J.Q. Liu, W. Zhao, G.L. Wen, J. Xu, X. Chen, Q. Zhang, Y. Wang, Y. Zhang, Y.C. Wu, Hydrothermal synthesis of well-standing δ-MnO2 nanoplatelets on nitrogen-doped reduced graphene oxide for high-performance supercapacitor. J. Alloy. Compd. **30**(787), 309–317 (2019)
23. H.A. Ghaly, A.G. El-Deen, E.R. Souaya, N.K. Allam, Asymmetric supercapacitors based on 3D graphene-wrapped V2O5 nanospheres and Fe3O4@ 3D graphene electrodes with high power and energy densities. Electrochim. Acta **1**(310), 58–69 (2019)